Clim Dyn (2012) 39:1697–1707
DOI 10.1007/s00382-012-1371-7

Precipitation variability during the past 400 years in the Xiaolong Mountain (central China) inferred from tree rings

Keyan Fang · Xiaohua Gou · Fahu Chen · David Frank · Changzhi Liu · Jinbao Li · Miklos Kazmer

Received: 10 June 2011 / Accepted: 16 April 2012 / Published online: 22 May 2012

Abstract We developed the first tree-ring chronology, based on 73 cores from 29 *Pinus tabulaeformis* trees, for the Xiaolong Mountain area of central China, a region at the boundary of the Asian summer monsoon. This chronology exhibits significant (at 0.01 level) positive correlations with precipitation in May and June, and negative correlations with temperature in May, June and July. Highest linear correlation is observed between tree growth and the seasonalized (April–July) precipitation, suggesting that tree rings tend to integrate the monthly precipitation signals. Accordingly, the April–July total precipitation was reconstructed back to 1629 using these tree rings, explaining 44.7 % of the instrumental variance. A severe drought occurred in the area during the 1630s–1640s, which may be related to the weakened Asian summer monsoon caused by a low land-sea thermal gradient. The dry epoch during the 1920s–1930s and since the late 1970s may be explained by the strengthened Hadley circulation in a warmer climate. The dry (wet) epochs of the 1920s–1930s (the 1750s and 1950s) occurred during the warm (cold) phases of the El Niño-Southern Oscillation and the Pacific Decadal Oscillation that are often associated with weakened (strengthened) East Asian summer monsoon. These relationships indicate significant teleconnections operating over the past centuries in central China related to large-scale synoptic features.

Keywords Tree ring · Precipitation · Central China · Asian summer monsoon · Dendroclimatology

Electronic supplementary material The online version of this article (doi:10.1007/s00382-012-1371-7) contains supplementary material, which is available to authorized users.

K. Fang (✉) · X. Gou (✉) · F. Chen · C. Liu
Key Laboratory of Western China's Environmental Systems (Ministry of Education), Research School of Arid Environment and Climate Change, Lanzhou University, Lanzhou 730000, China
e-mail: kyfang@lzu.edu.cn

X. Gou
e-mail: xhgou@lzu.edu.cn

K. Fang
Department of Geosciences and Geography, University of Helsinki, PO Box 64, 00014 Helsinki, Finland

D. Frank
Swiss Federal Research Institute WSL, Zürcherstrasse 111, 8903 Birmensdorf, Switzerland

D. Frank
Oeschger Centre for Climate Change Research, University of Bern, Bern, Switzerland

J. Li
International Pacific Research Center, School of Ocean and Earth Science and Technology, University of Hawaii at Manoa, Honolulu, HI 96822, USA

M. Kazmer
Department of Palaeontology, Eotvos University, Pazmany setany 1/c, Budapest 1117, Hungary

1 Introduction

To improve our understanding of the earth's climate system, assess impacts of climate change, and differentiate natural versus anthropogenic climate variability, it is necessary to develop temperature and hydroclimate reconstructions extending beyond the industrial-era across the globe (Jones et al. 2009). Only with such reconstructions could we benchmark global change phenomena in a long-term context. For example, a compilation of large-scale temperature reconstructions shows that recent warming has

already increased the pre-industrial amplitude of temperature variability by 75 %, though regional features and impacts associated with both past and future climate variability are still subjected to considerable uncertainties (IPCC 2007). These uncertainties are particularly large for hydroclimate change due to its spatial heterogeneity and sensitivity to different circulation patterns (Schiermeier 2010). In this study we address these knowledge gaps and present a new evidence of past hydroclimate change for a data sparse region in central China.

Xiaolong Mountain is located in the western part of the Qinling Mountains, an important east–west geographic boundary that divides the southern and the northern central China. Our study region in the Xiaolong Mountain area is located in the marginal zone influenced by the Asian summer monsoon, where regional climate regime is highly sensitive to global climate change (Chen et al. 2008). Xiaolong Mountain is also a transitional area between dense vegetation coverage to the southeast and sparse vegetation coverage to the north and west, as indicated by a sharp gradient in Normalized Difference Vegetation Index (NDVI) values (Fig. 1). Impacts of climate change on forests are generally more evident at their distribution limits (Esper and Schweingruber 2004), requiring deeper knowledge on how climate has varied in these boundary regions in the past. In central China instrumental records are generally available since the 1950s, prohibiting a comprehensive evaluation of pre-industrial climate variation. The annual growth rings of trees are a particularly useful climate proxy due to their annual resolution, climate sensitivity and widespread availability (Fritts 1976). Several tree-ring based drought reconstructions have been developed for neighboring regions in north central China (Hughes et al. 1994; Li et al. 2007; Liu et al. 2004). Yet, there is no tree-ring chronology published for the Xiaolong Mountain, an area mainly covered by secondary forests with limited old-growth woods. Here we present the first tree-ring chronology (AD 1607–2009) for the Xiaolong Mountain area using samples from the old-growth Chinese pine (*Pinus tabulaeformis*) trees, and employ these data to reconstruct regional precipitation variability.

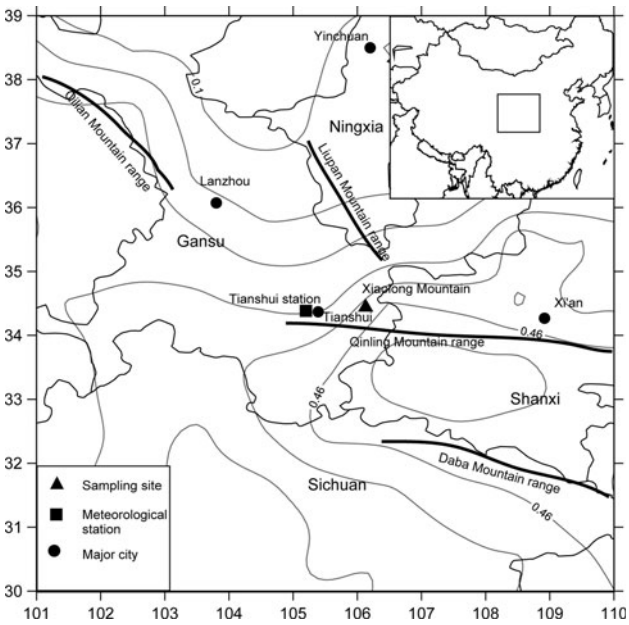

Fig. 1 Locations of the sampling site at Xiaolong Mountain, meteorological station and major cities in the study region in central China, as well as the *contours* indicating the averaged April–June NASA pathfinder Normalized Difference Vegetation Index (NDVI) for the period 1982–2001. The NDVI data was derived from the Advanced Very High Resolution Radiometer (AVHRR) with a spatial resolution of 1° × 1° (http://disc.sci.gsfc.nasa.gov/)

2 Data and methods

2.1 Study region

Our research area in Xiaolong Mountain (104.37–106.71°E; 33.50–34.82°N, 700–3,330 m a.s.l.) is located in central China, a marginal area of Asian summer monsoon (Fig. 1). This is also a transitional area between the Yellow River and the Yangtze River valleys in northern and southern China, respectively. Abundant forest coverage is found in the southeastern area of the Xiaolong Mountain area (Fig. 1), which is caused by the southeastly moisture flux. At the same time, increased precipitation and reduced evaporation caused by topography effects favor tree growth in this semi-arid region. Additionally, special attention should be paid to the underlying surface and soil conditions in China's Loess Plateau. For example, the mountain areas with a rocky-base have a greater capacity to retain soil moisture, in comparison to the porous loess. As a result, the "green islands" often coincide with "rocky islands", such as the Xinglong Mountain (35.82°N, 104.07°E), the Guiqing Mountain (34.63°N, 104.47°E) and the Kongtong Mountain (35.54°N, 106.51°E).

The annual mean temperature in the area is 10.9 °C and the annual total precipitation is 518.5 mm, according to the meteorological records from the nearest station at Tianshui (34.35°N, 105.45°E, 1,141.7 m a.s.l.) from 1951 to 2003. As shown in Fig. 2, the highest monthly mean temperature is in July (22.8 °C) followed by August (21.8 °C) and June (20.7 °C), and the monthly total precipitation peaks in July (91.7 mm) followed by September (86.4 mm) and August (84.7 mm).

2.2 Tree-ring chronology

Tree cores from *P. tabulaeformis* were collected at two proximally-located sites (34.45°N, 106.13°E), the "north peak" and "south peak" sites in the northern part of the

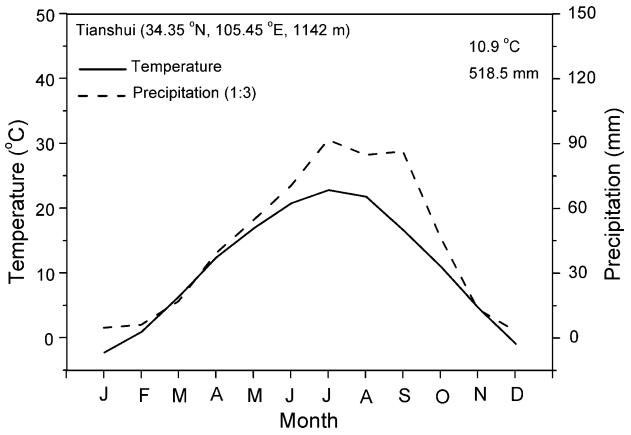

Fig. 2 Walter climate diagram for the Tianshui meteorological station showing the (*solid line*) monthly mean temperature and monthly precipitation (*dashed line*) with a 1:3 ratio between *y*-axis of temperature and precipitation

Xiaolong Mountain (Fig. 1). *P. tabulaeformis* is not the dominant tree species in the Xiaolong Mountain area and is only found in rocky areas near cliffs or around temples. There are small areas of pure and open pine woods at the mountain peaks. The local inhabitants favor pine trees and often plant some near temples, providing sufficient seeds for neighboring regions with shallow soil of limited suitability for tree growth. Trees growing on steep slopes or cliffs generally have more branches on the downslope side, regardless of the direction of sunlight or wind. This may be because soil condition is better over the downslope side, providing relatively sufficient water and nutrients for the generation of branches downslope. Reaction wood is often developed in the trees with more branches, which could support the trees. This is widely seen for the gymnosperms trees with reaction wood downslope to support trees growing on slopes (Fritts 1976).

Two to four cores were sampled from each tree from different directions, and were subsequently dried, mounted and sanded in lab (Cook and Kairiukstis 1990). Tree-ring from both the "north peak" and "south peak" sites were crossdated using skeleton plots in order to assign a correct calendar year to each ring. The subsequently measured series with a 0.001 mm precision were checked using the program COFECHA (Holmes 1983) for the quality control of crossdating. The ring-width sequences from both sites were found to be highly correlated at this stage, indicative of a common climate signal. It has been suggested that tree-ring series growing within one site may show different climate-growth associations due to micro-environmental conditions (Frank and Esper 2005; Meko 1997; Wilmking et al. 2005). For example, tree rings in shaded or concave locations with relatively abundant moisture availability in arid regions may be less sensitive to moisture. We thus also examined the homogeneity in climate-growth correlations among tree-ring sequences prior to the establishment of a chronology. Three cores sampled from trees with branches cut off or deep soil showed non-significant correlations to either temperature or precipitation, which were excluded from further analyses. We note that chronologies including or excluding these cores agree well with each other, indicating that the effects of this screening are minimal. We removed the age-related trend and translated the tree-ring series to dimensionless tree-ring indices by fitting the measured values with a 100-year spline.

Fitted curves in traditional detrending method may be distorted by the climate signals and thus result in biased chronology indices (Melvin and Briffa 2008). This socalled "trend distortion problem", the localized standardization distortions, can be at least mitigated by employing a "signal free" detrending method (Melvin and Briffa 2008). This problem was observed in our tree-ring chronology when using the traditional method (details in the Sect. 3). We thus employed the "signal-free" method to develop the tree-ring chronology. That is, tree-ring indices were first calculated as ratio between raw measurements and the initial fitted curves. The climate variation represented in the final chronology was removed from the raw tree-ring measurement series by division, and then the age-related trend was again estimated. This procedure is iterated until the "signal-free" detrending curves do not change, and thus provides a best estimate of the age-related trend free of climate influences (Melvin and Briffa 2008). Since there is minor difference between the ecological features of the "north peak" and "south peak" sites that are about 1 km away from each other, we generate a composite chronology using tree-ring cores from both sites. That is, tree-ring indices from 70 cores, 31 cores of 12 trees taken at the "north peak" site and 29 cores of 18 trees sampled from the "south peak" site, were averaged with a robust biweight mean method (Cook 1985) to produce a composite chronology.

3 Results

The final chronology, spanning from 1607 to 2009 with a mean segment length of 185.7 years, was developed with five "signal-free" iterations. The signal-free method results in some subtle changes to the final chronology in comparison to the conventional detrending. As shown in Fig. 3, the below average chronology indices (dark line) during the 1630s–1650s and 1730s–1750s became more extreme after the signal-free iterations. These differences make sense because the "trend distortion" problem tends to dampen the medium-frequency variability by, for example, increasing the below average indices or lowering the above-than-normal indices (Melvin and Briffa 2008).

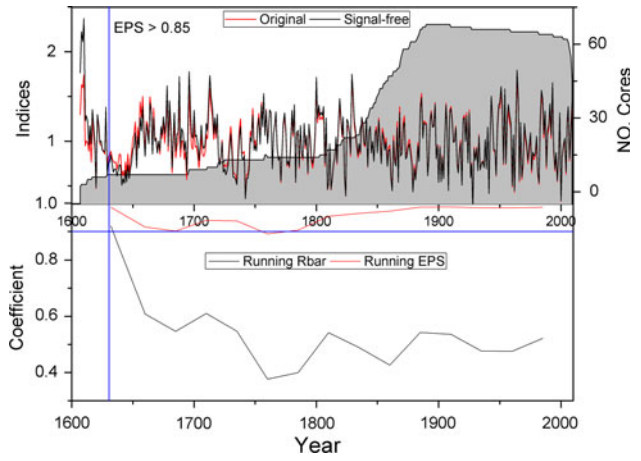

Fig. 3 The (*upper panel*) chronology indices before (*red line*) and after (*black line*) signal-free iterations, as well as the running Rbar (running for based upon a 50-year window lagged 25 years) and statistics of the running expressed population signal (EPS). The reliable portion of the chronology is determined by the EPS value greater than 0.85

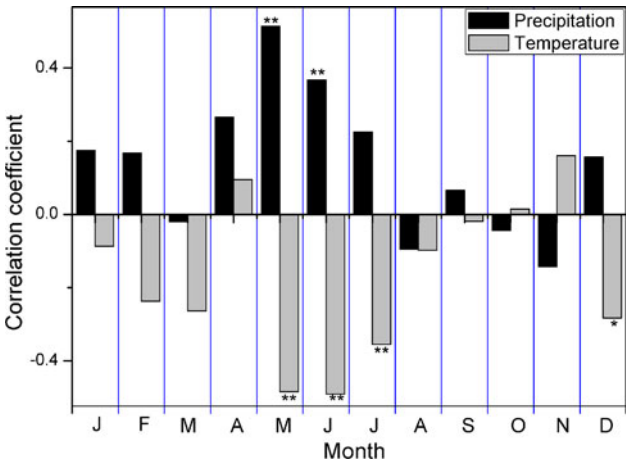

Fig. 4 Correlations between tree-ring indices at Xinglong Mountain and (*black bar*) precipitation and (*grey bar*) temperature of the nearby station at Tianshui from January to December during the period from 1951 to 2003. The 95 and 99 % significance levels are indicated by *one* and *two asterisks*, respectively

However, the "signal-free" method alone does not aim at distinguishing the climate-related growth signals from the inherent age-related trends, thereby showing no special ability to retain the low-frequency climate signals (Melvin and Briffa 2008). Thus we remain cautionary in addressing the low-frequency climate variability that may exist on time-scales longer than the segment length of our dataset (Cook et al. 1995). Running Rbar (moving correlations among series) and running expressed population signal (EPS) values are generally high (Fig. 3), indicating reliable chronology signal strength through time (Wigley et al. 1984). The following analyses are only based on the reliable portion of the chronology spanning from 1629 to 2009, which is determined by the EPS value greater than 0.85 (Wigley et al. 1984).

As shown in Fig. 4, significant ($p < 0.01$) positive Pearson correlations between tree growth and precipitation from 1951 to 2003 are found in May (0.514) and June (0.367), and significant ($p < 0.01$) negative correlations with temperature are seen in May (−0.485), June (−0.491) and July (−0.355). Highest linear correlation is found between the April–July total precipitation and tree growth. We accordingly reconstructed the April–July total precipitation from 1629 to 2003, which explains 44.7 % of the instrumental variance during the 1951–2003 period (Fig. 5a). The reconstruction was scaled to have equal mean and variance with the instrumental data during the 1951–2003 common period. The error ranges measure the uncertainties of the reconstruction due to the signal strength of the tree-ring chronology. The reconstruction model is stable over time as indicated by the split period calibration-verification tests (Table 1). These validation trials were performed by calibrating climate data from one period (1951–1980 and 1974–2003) and verifying the reconstruction using the remaining data (1981–2003 and 1951–1973), a method commonly used to test model reliability (Li et al. 2007). The high explained variance and both the reduction of error (RE) and coefficient of efficiency (CE) statistics with values greater than zero (Table 1) indicate acceptable reconstruction reliability. The final reconstruction shown in Fig. 5b is based upon calibration to the full period of instrumental data.

4 Discussion

4.1 Climate-growth relationships

Drought-stress appears to be the dominant climate limitation for the *P. tabulaeformis* tree growth in the Xiaolong Mountain area, as indicated by positive correlations with precipitation and negative correlations with temperature. As indicated by the Walter climate diagram in Fig. 2, a drought-stressed growing pattern is observed in the growing season (e.g. June and July) because precipitation is less abundant relative to temperature. The high (low) June temperature could intensify (weaken) evapotranspiration and result in narrow (wide) ring when precipitation is less abundant. This drought-stress growth pattern during the growing season is widely documented in nearby regions, such as the Xinglong Mountain (Fang et al. 2009), Helan Mountain (Li et al. 2007), and the Guiqing Mountain (Fang et al. 2010b). It is readily understood that drought limitation is more intense before July due to the asymmetric distribution of monthly precipitation with less precipitation

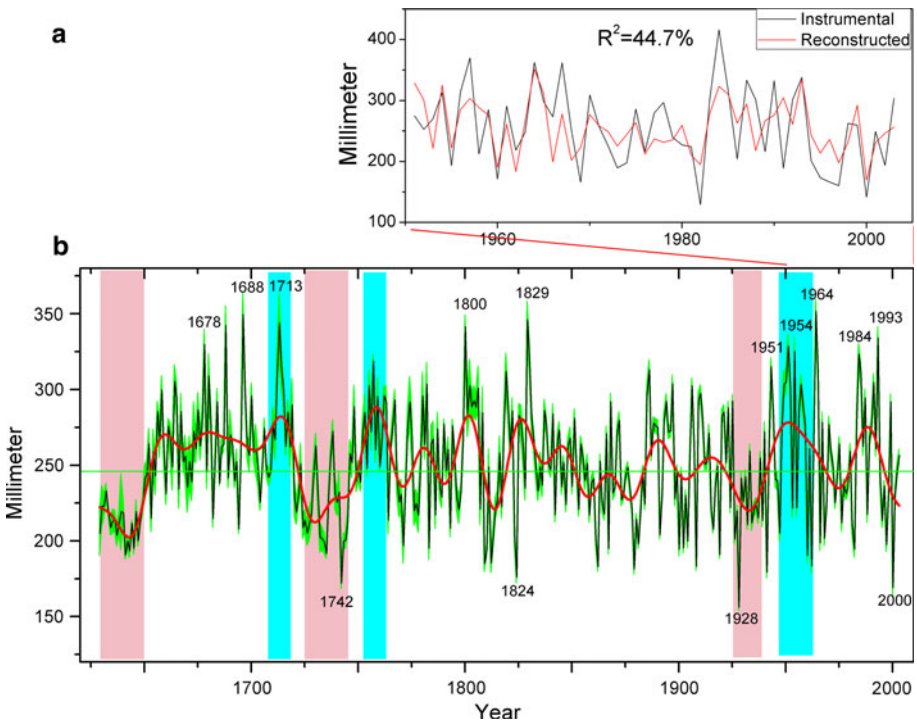

Fig. 5 **a** The (*upper panel*) comparisons between the (*red line*) instrumental and (*dark line*) reconstructed April–July precipitation and **b** the (*dark thin line*) reconstructed precipitation from 1629 to 2003 and the (*red bold line*) 20-year low passed data. The (*green shaded area*) error ranges were derived from the signal strength of the tree-ring chronology

Table 1 Statistics of the split calibration-verification model for the precipitation reconstruction at Xiaolong Mountain

	Calibration (1951–1980)	Verification (1981–2003)	Calibration (1974–2003)	Verification (1951–1973)	Calibration (1951–2003)
r	0.637	0.715	0.677	0.666	0.668
R^2	0.406	0.511	0.458	0.444	0.447
RE		0.444		0.411	
CE		0.426		0.359	

r correlation coefficient, R^2 explained variance, *RE* reduction of error, *CE* coefficient of efficiency

in the early half of the year. Moreover, the early wood cells formed during the early growing season represent the majority of the total ring-width. Such drought sensitive climate-growth relationship is often associated with stronger correlations with the Palmer Drought Severity Index (PDSI), a direct metric of local moisture conditions (Dai et al. 2004). Our tree-ring samples, however, show lower correlations with PDSI than with temperature and precipitation (results not shown). The low PDSI-growth correlation may be an indicator of degraded quality of PDSI data at this grid, which is less representative of local drought conditions in the Xiaolong Mountain. The drought sensitive tree rings over the mountainous regions might be considered useful references for the verification of gridded climate data in mountainous areas where limited instrumental records are available. While this appears quite speculative to use tree rings to test instrumental records, in Asia, similar tree-ring/climate assessments helped pinpoint inhomogeneities remaining in the long instrumental records (Cook and Pederson 2011).

Higher correlations were observed between tree rings and seasonalized precipitation compared to correlations for individual months, indicating potential nonlinearity in climate-growth relationships for individual months. In order to test the nonlinearity in the relationships between tree growth and climate of individual month, we herein employed the feed-forward backward-propagation artificial neural network (ANN) method to examine the climate-growth relationships, a method widely used in dendroclimatology to detect and model the nonlinear climate-growth relationships (Guiot et al. 2005; Ni et al. 2002; Woodhouse 2001; Zhang et al. 2000). Detailed introductions to the ANN method and the design of the network are given in the Appendix: Electronic Supplementary Material. We herein trained the ANN model by simulating tree growth with the use of six input monthly climate variables (i.e. mean April–May temperature, mean temperature in June and July, monthly total April–May precipitation, and June and July precipitation) that show relatively high correlations with tree growth. The trained ANN model is used to simulate

tree-ring indices under different combinations of input precipitation and temperature. These simulations are designed to test the changes in the climate-growth relationships under different scenarios of climate conditions. Linearity in climate-growth relationships is found in relatively high (low) April–May total precipitation and low (high) June total precipitation (Fig. 6a). This reflects a physiological "compensation" and/or opportunistic growth strategy related to water availability. High (low) precipitation in both April–May and June may exceed the high (low) threshold for the linear relationships. A similar "compensation" feature was observed between June and July precipitation (Fig. 6b). Tree growth integrates monthly precipitation from April to July and better models the linear associations with the April–July total precipitation. There is limited difference between the linear and nonlinear reconstructions of the April–July total precipitation (Figure S1). This is because tree growth is linearly correlated with April–July total precipitation and thus both the linear and nonlinear reconstruction models are mainly based on the linear relationship. We thus consider that the linear reconstruction is able to recover the seasonalized precipitation.

The strength of the linear precipitation-growth relationship decreases in extreme climate conditions (Fig. 6). A generally accepted view is that drought-stressed trees show limited ability in recording extreme wet conditions (Fritts 1976). In fact, the predominantly linear climate-growth relationships might change in extremely dry or wet conditions beyond a certain threshold. Our ANN modeling result is in agreement with the "principle of the ecological amplitude", with similarly inverted U-shaped curves of climate-growth interactions. Linear, negative associations between June temperature and tree growth are observed when June precipitation ranges from ~125 to ~200 mm (Fig. 6c). This feature can be understood intuitively because the increase in temperature accompanies an increase in evapotranspiration that could limit tree growth. This provides another evidence that tree rings are sensitive to moisture, and the temperature-growth relationships are likely indirect via a modification of evapotranspiration.

It is expected that the uncertainties of the linear reconstruction could increase in extreme climate conditions when linearity of the precipitation-growth association decreases. Figure 6a shows that the tree-ring indices increase linearly

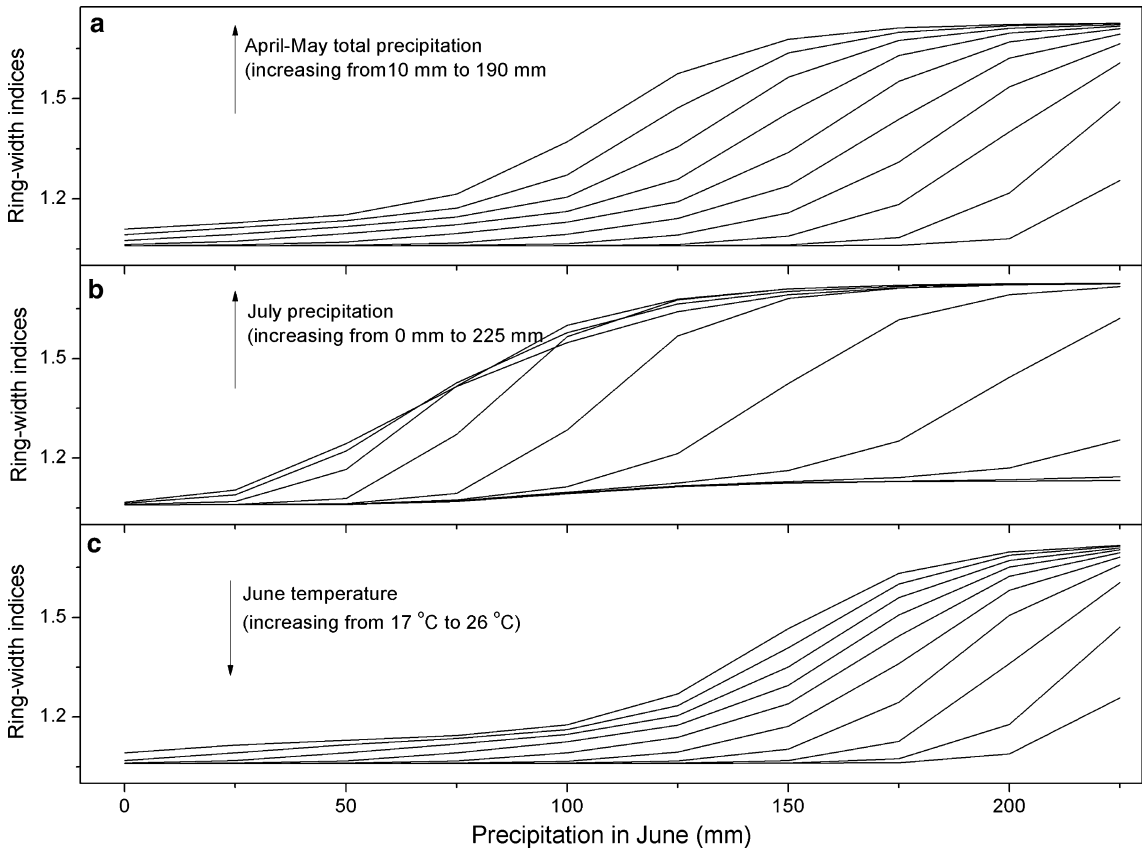

Fig. 6 The artificial neural network (ANN) simulated ring-width indices from June precipitation increasing from 0 to 225 mm associated with **a** April–May total precipitation increasing from 10 to 190 mm, **b** July precipitation increasing from 0 to 225 mm and **c** June temperature increasing from 17 to 26 °C. The ANN was trained using precipitation and temperature records during the instrumental period 1951–2003 and the concurrent ring-width indices

when the sum of April–May precipitation and June precipitation is between ~200 and ~300 mm. Similarly, tree growth increases linearly with June and July precipitation in a few scenarios when July precipitation is from ~75 to ~125 mm (Fig. 6b). Although it is difficult to provide a quantitative measure (e.g. error bars) of the reconstruction uncertainties due to the potential nonlinearity in climate-growth relationships, we simply calibrated different linear reconstruction models by only using the extreme or moderate precipitation values. As shown in Figure S2, the reconstruction amplitude using the entire instrumental data is between the reconstruction using extreme values and the one derived from moderate values. The amplitude between the reconstructions is large for the extreme reconstructed values and is narrow for the moderate values, consistent with the above finding that the uncertainties increase for the extreme values. This method and finding represents a further factor that contributes to the "*y*-axis" amplitude uncertainties related to the calibration of the proxy data (Frank et al. 2010). There are uncertainties inherent to the arguably arbitrary criteria (herein greater or lower than mean + SD) to divide the extreme and moderate values. The short length of the extreme and moderate instrumental data could also lead to errors or bias in proxy calibration. At this point there seems to be no clear or best solution to reduce these uncertainties. Pending further research, we advocate, to the extent possible, using climate and proxy data that cover the full data range found in the climate and proxy records. We further infer that a reconstruction derived from a calibration period with only extreme (moderate) values could be less reliable, because the reconstructed values may overestimate (underestimate) the reconstruction variability. In other words, a reliable reconstruction model should be calibrated using climate and tree-ring data that cover the full range of the data over the entire reconstruction period. The reconstruction uncertainties could also be associated with the signal strength of the tree-ring chronology that is mainly dependent on the sample size. Error ranges of the reconstruction become narrow towards recent with the increase of the number of tree-ring samples (Fig. 5b), which tends to increase the signal strength of a tree-ring chronology (Fritts 1976).

4.2 Drought variations and potential climate regimes

April-July precipitation reconstruction in the Xiaolong Mountain area exhibits variability at interannual to centennial time-scales. Significant ($p < 0.01$) spectral peaks were found at ~2–3 years (Fig. 7). We also identified cyclic patterns ($p < 0.1$) at 3.4–3.5, 3.7–3.8, 6.6–6.7, 6.9, 8.9, 19.7, 22.3, 40.9–56.8 and 85.5–102.0 years. The 2–3 year cyclic precipitation variability in the Xiaolong Mountain area was widely documented in previous tree-ring based climate reconstructions (Fang et al. 2010b; Li et al. 2007), which may be related to the tropospheric biennial oscillation (TBO) (Meehl and Arblaster 2010). The spectral peaks of 3.4–6.9 years fall within the spectral bandwidth of the El Niño-Southern Oscillation (ENSO). ENSO variability was documented to modulate the strength of Asian summer monsoon (Lu 2005; Zhang et al. 1999), resulting in precipitation changes in the marginal monsoon areas such as the Xiaolong Mountain. The decadal variability at spectral peaks of 19.7–22.3 years and 56.8 years may be related to the Pacific Decadal Oscillation (PDO) (Mantua et al. 1997), which can modify the strength of both the winter and summer Asian monsoon (Li et al. 2004).

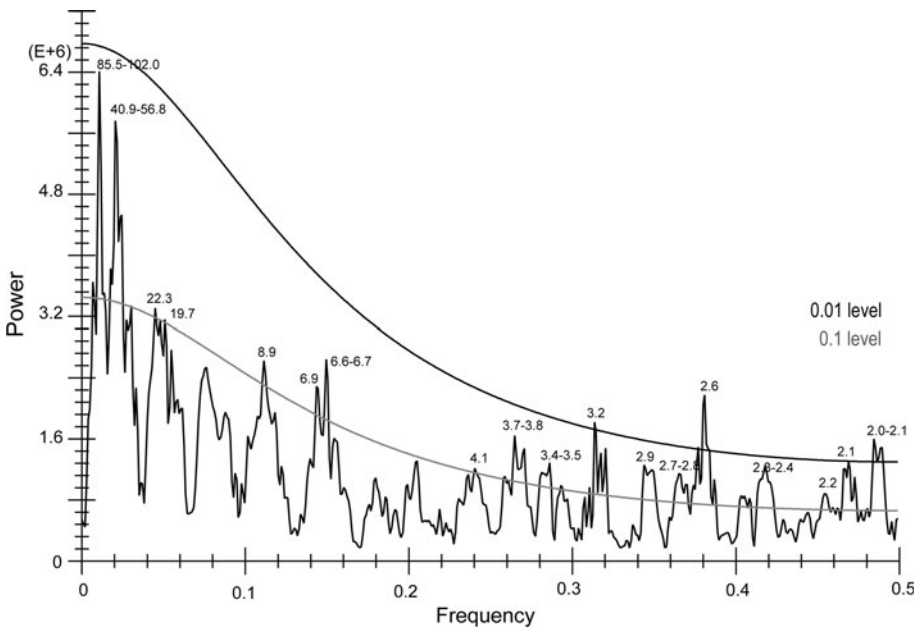

Fig. 7 Multi-taper spectrum of the reconstruction and their confidence limits at the 0.01 (*solid line*) and 0.1 levels (*light*)

The mean value and standard deviation (SD) of the April-July reconstruction are 248 and 54 mm, respectively, and serve as useful benchmarks to evaluate long term precipitation variability in the region.

Dry epochs with 10 persistent dry (<average − 1 SD) summers, based on a 20-year low-passed filtered data, are found for the 1630s–1640s, 1730s–1740s, 1920s–1930s and since 1970s. Epochs with 10 persistent wet (>average + 1 SD) summers are reconstructed for the 1710s, 1750s and 1950s. The dry epoch during the 1630s–1640s (Fig. 5b), concomitant with the collapse of the Chinese Ming Dynasty (Zhang et al. 2008), corresponds with severe dry conditions in previous tree-ring based drought reconstructions for northern China (Cook et al. 2010; Fang et al. 2010a) and low values in a stalagmite oxygen isotope series south to the Xiaolong Mountain area (Fig. 8). This drought was considered the most extreme in China over the past five centuries (Cook et al. 2010; Shen et al. 2007). The 1630s–1640s drought also coincided with the coldest period over the past five centuries in China as inferred from a speleothem-based temperature reconstruction for the Beijing area (Tan et al. 2003) and a multi-proxy (ice cores, tree rings, peat and historical documents) temperature reconstruction for China (Yang et al. 2002). The cold and dry extreme conditions suggest potential linkages between temperature variability and the strength of Asian monsoon, which is closely related to precipitation variability in the monsoon marginal area including the Xiaolong Mountain. Low (high) temperature could result in reduced (increased) land-sea thermal contrast and thus lead to a weakened (strengthened) Asian summer monsoon (Zhang et al. 2008). In addition, the seventeenth century dry epoch occurred during a warm phase of PDO (D'Arrigo and Wilson 2006), which tends to be associated with weakened eastern Asia summer monsoon (Li et al. 2004). After this dry epoch, persistent wet conditions were observed during the latter half of the seventeenth century. The persistent wetness was also found in neighboring regions such as the Guiqing mountain area (Fang et al. 2010b). This wetness may be related to the rising trend in temperature during the latter half of the seventeenth century (Yang et al. 2002), which could increase the land–ocean thermal gradient and the strength of monsoon.

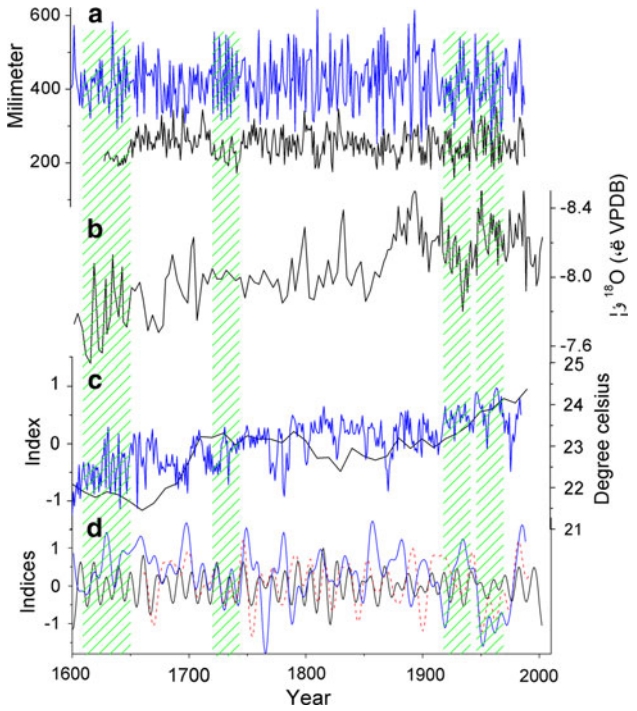

Fig. 8 Comparisons of climate reconstructions **a** between this (*dark line*) April–July total precipitation reconstruction and the (*blue line*) April–July precipitation reconstruction at central Qinling Mountain eastern to the study region (Hughes et al. 1994), **b** a monsoon proxy from a speleothem record at Wanxiang cave southern to the study region (Zhang et al. 2008), **c** temperature reconstruction from a (*blue line*) speleothem record at Beijing (Tan et al. 2003) and (*dark line*) mean temperature index for China from multiple proxies of ice cores, tree rings, peat and historical documents (Yang et al. 2002), as well as **d** a (*dark line*) ENSO reconstruction by Li et al. (2011), the (*blue line*) 10-year low passed PDO reconstruction using tree rings of North America by Biondi et al. (2001) and the (*red* and *dashed line*) Asian expression of PDO by D'Arrigo and Wilson (2006)

Hydroclimate conditions were variable in the eighteenth century, with the wet epochs in the 1710s and 1750s and the dry epochs in the 1730s–1740s (Fig. 5b). These wet and dry epochs were also observed in nearby regions (Fang et al. 2010b) and in northeastern Mongolia (Pederson et al. 2001), suggesting widespread spatial teleconnections. This may be because both the northeastern Mongolia and the study region are located near the boundary of the monsoonal Asia (Chen et al. 2008) and thus may show similar drought variations in associations with the dynamics of Asian monsoon. A coherent moisture pattern covering the northeastern Mongolia, northeastern China and north central China was revealed by a previous study (Li et al. 2009). Our reconstruction in the Xiaolong Mountain area and the reconstructions in northeastern Mongolia are located within that large-scale drought pattern, lending further support for this empirical pattern during the past centuries. The wet (dry) epochs occurred during the 1710s and 1750s (1730s–1740s) coincide with the relatively warm (cold) conditions (Tan et al. 2003; Yang et al. 2002), which tends to be accompanied by intensified monsoon. In addition, the wet epochs during the 1710s and 1750s occurred during the cold phases of both the PDO (Biondi et al. 2001) and ENSO (Li et al. 2011). East Asian summer monsoon tends to be weakened (intensified) during the warm (cold) phase of the PDO and ENSO variability (Lu 2005; Su and Wang 2006; Zhang et al. 1999), which also tends to result in a drought (wetness) in our study region.

The 1920s–1930s drought, a widely recorded event in northern China that resulted in the death of at least four million people (Liang et al. 2006), was found in a number of previous tree-ring reconstructions in marginal areas of Asian monsoon, such as the central China (Fang et al. 2009, 2010b; Hughes et al. 1994; Li et al. 2007) and the northeastern Mongolia (Pederson et al. 2001). However, as shown in Fig. 8, the 1920s–1930s drought occurred during a relatively warm period in China (Tan et al. 2003; Yang et al. 2002) and is characterized by an abrupt warming trend since the 1920s for the Northern Hemisphere (Fu et al. 1999), suggesting other factors also influence the monsoon strength in addition to the land–sea thermal gradients. For example, this drought in the 1920s–1930s occurred during a warm phase PDO (Biondi et al. 2001; D'Arrigo and Wilson 2006) and ENSO (Li et al. 2011), both of which tend to be associated with strengthened eastern Asia summer monsoon. This dry epoch may also be related to the weakened Indian summer monsoon during that period, as indicated by the relatively low Indian monsoon rainfall during the period of 1895–1932 (Sontakke and Singh 1996; Sontakke et al. 2008). In addition, this relatively warm period may be associated with the strengthened Hadley circulation (Fu et al. 1999). The intensified downward limb of the Hadley circulation caused dry conditions in subtropical areas, such as this drought epoch in northern China and the dust bowl drought during the 1930s in North America (Cook et al. 2004).

In the latter half of the twentieth century, persistent wet conditions in the 1950s and the drying trend since late 1970s were observed. The wet epoch in the 1950s was observed in several previous drought reconstructions in northern China (Hughes et al. 1994) and northeastern Mongolia (Pederson et al. 2001), and was found to cover a large spatial area (Fang et al. 2010a; Li et al. 2009). This wetness occurred during the cold phase of both the PDO and the ENSO (Fig. 8). The Indian summer monsoon was strong during this period (Sontakke and Singh 1996; Sontakke et al. 2008), which may contribute to this wet epoch. The drying tendency since the late 1970s was also documented in nearby regions (Fang et al. 2010a; Li et al. 2007), which coincides with the weakening of the Asian summer monsoon in recent decades (Cook et al. 2010; Goswami et al. 2006; Sontakke and Singh 1996; Sontakke et al. 2008; Zhang et al. 2008). This dry epoch may also be associated with similar mechanisms as that in the 1920s–1930s, namely the intensified Hadley cell due to a warmer climate (Fu et al. 2006). In addition, the intensified anthropogenic forcings may have played an important role on the strength of the Asian summer monsoon (Zhang et al. 2008). For example, the spatial distribution of the sulfate aerosols was documented to shift the monsoon rainfall southward, which tends to reduce the monsoon rainfall at its shoulder regions (Zhang et al. 2008) including our study region. On the other hand, deforestation due to intensified cultivation activities in recent decades in this semi-arid region may also contribute to the drying trend. For example, many trees were cut down for industrial activities, such as the production of iron and steel during the late 1950s to the early 1960s (http://www.china.org.cn/english/features/47599.htm). The drying tendency could in turn strengthen the warming trend, because insufficient water availability may reduce evapotranspiration and latent heat flux from earth's surface, thereby increasing warming (Wang et al. 2007). Collectively, these results indicate how new long term records from data sparse region can play an important role in assessing both stability and shift in large ocean-atmospheric circulation patterns. With more proxy reconstructions extending our knowledge of pre-industrial climate variability, we will be able to better differentiate the responses of climate systems to natural from anthropogenic forcings.

5 Conclusions

In this study, we developed a tree-ring based precipitation reconstruction to improve quantification and understanding of the climate regime in the Xiaolong Mountain area, a border area of the Asian summer monsoon in central China. Using the "signal-free" detrending method with five iterations, we established the first tree-ring chronology for the Xiaolong Mountain area that spans from 1607 to 2009. Significant positive correlations between tree growth and precipitation were found in May and June, while negative correlations with temperature were found in May, June and July. Trees tend to integrate precipitation signals of consecutive months (April–July) and can "compensate" short-term (e.g., monthly) water shortages or surpluses to maintain annual growth. As a result, seasonally averaged precipitation shows higher linear correlations with tree growth, relative to monthly precipitation. There are further uncertainties in the calibration of proxy that will need more methodological attention in the future. For now, we recommend using the full instrumental period data and consider both the extreme and moderate conditions when calibrating proxy data.

Using the reliable period (1629–2009) of the chronology, we reconstructed April-July total precipitation with a model explaining 44.7 % of the instrumental variance. Precipitation in the Xiaolong Mountain area, a shoulder-region of the Asian summer monsoon, is sensitive to the strength of the Asian monsoon, and the dry/wet epochs generally indicate the weakened/intensified Asian monsoon. Decadal-scale dry (wet) epochs during the periods of the 1730s–1740s and 1920s–1930s (1710s, 1750s and 1950s) were also found in nearby regions and northeastern

Mongolia, suggesting the coherent drought regimes over these marginal areas of the monsoonal Asia. The dry (wet) epochs during the periods of 1630s–1640s and 1730s–1740s (1710s and 1750s) occurred during the cold (warm) period, which may be caused by reduced land–ocean thermal gradients and the weakened monsoon. The dry epochs of the 1920s–1930s and the drying trend since the late 1970s occurred during the relatively warm periods, which may be associated with the strengthened Hadley circulation in a warmer climate. The intensified Hadley cell could suppress the convection in the Xiaolong Mountain area and lead to dry conditions. The dry (wet) epochs in the 1920s–1930s (1710s, 1750s and 1950s) occurred during the warm (cold) phases of both the PDO and ENSO, which tends to be associated with weakened (intensified) Asian monsoon. Our reconstruction has provided new quantification of the past changes in moisture regimes and allowed insights into the externally forced and ocean–atmosphere modes that contribute to precipitation variability in central China.

Acknowledgments The authors acknowledge the kind assistances from Dongju Zhang and Zhiqian Zhao. This research was supported by the National Basic Research Program of China (2012CB955301), the National Science Foundation of China (41001115 and 40971119), the Chinese 111 Project (B06026), and Hungarian NSF grant K 67.583. DCF acknowledges support from the Swiss National Science Foundation (NCCR-Climate, DE-TREE).

References

Biondi F, Gershunov A, Cayan DR (2001) North Pacific decadal climate variability since 1661. J Clim 14:5–10

Chen F, Yu Z, Yang M, Ito E, Wang S, Madsen DB, Huang X, Zhao Y, Sato T, John BB (2008) Holocene moisture evolution in arid central Asia and its out-of-phase relationship with Asian monsoon history. Quat Sci Rev 27:351–364

Cook ER (1985) A time series analysis approach to tree ring standardization. PhD. The University of Arizona, Tucson

Cook E, Kairiukstis L (1990) Methods of dendrochronology: applications in the environmental science. Kluwer, Dordrecht

Cook ER, Pederson N (2011) Uncertainty, emergence, and statistics in dendrochronology. In: Hughes MK, Swetman TW, Diaz H (eds) Dendroclimatology: Progress and prospects. Springer, Berlin, pp 77–112

Cook ER, Briffa KR, Meko DM, Graybill DA, Funkhouser G (1995) The 'segment length curse' in long tree-ring chronology development for palaeoclimatic studies. Holocene 5:229–237

Cook E, Woodhouse CA, Eakin CM, Meko DM, Stahle DW (2004) Long-term aridity changes in the western United States. Science 306:1015

Cook E, Anchukaitis KJ, Buckley BM, D'Arrigo RD, Jacoby GC, Wright WE (2010) Asian monsoon failure and megadrought during the last millennium. Science 328:486–489

Dai A, Trenberth KE, Qian T (2004) A global dataset of Palmer Drought Severity Index for 1870-2002: Relationship with soil moisture and effects of surface warming. J Hydrometeorol 5:1117–1130

D'Arrigo R, Wilson R (2006) On the Asian expression of the PDO. Int J Climatol 26:1607–1617

Esper J, Schweingruber FH (2004) Large-scale treeline changes recorded in Siberia. Geophys Res Lett 31:L06202. doi: 10.1029/2003GL019178

Fang K, Gou X, Chen F, Yang M, Li J, He M, Zhang Y, Tian Q, Peng J (2009) Drought variations in the eastern part of Northwest China over the past two centuries: evidence from tree rings. Clim Res 38:129–135

Fang K, Davi N, Gou X, Chen F, Cook E, Li J, D'Arrigo R (2010a) Spatial drought reconstructions for central High Asia based on tree rings. Clim Dyn 35:941–951

Fang K, Gou X, Chen F, D'Arrigo R, Li J (2010b) Tree-ring based drought reconstruction for the Guiqing Mountain (China): linkages to the Indian and Pacific Oceans. Int J Climatol 30:1137–1145

Frank D, Esper J (2005) Temperature reconstructions and comparisons with instrumental data from a tree-ring network for the European Alps. Int J Climatol 25:1437–1454

Frank DC, Esper J, Raible CC, Büntgen U, Trouet V, Stocker B, Joos F (2010) Ensemble reconstruction constraints on the global carbon cycle sensitivity to climate. Nature 463:527–530

Fritts HC (1976) Tree rings and climate. Academic Press, New York

Fu C, Diaz HF, Dong D, Fletcher JO (1999) Changes in atmospheric circulation over Northern Hemisphere oceans associated with the rapid warming of the 1920s. Int J Climatol 19:581–606

Fu Q, Johanson CM, Wallace JM, Reichler T (2006) Enhanced mid-latitude tropospheric warming in satellite measurements. Science 312:1179

Goswami BN, Venugopal V, Sengupta D, Madhusoodanan MS, Xavier PK (2006) Increasing trend of extreme rain events over India in a warming environment. Science 314:1442

Guiot J, Nicault A, Rathgeber C, Edouard JL, Guibal F, Pichard G, Till C (2005) Last-millennium summer-temperature variations in western Europe based on proxy data. Holocene 15:489

Holmes RL (1983) Computer-assisted quality control in tree-ring dating and measurement. Tree Ring Bull 43:69–78

Hughes MK, Xiangding W, Xuemei S, Garfin GM (1994) A preliminary reconstruction of rainfall in north-central China since AD 1600 from tree-ring density and width. Quat Res 42:88–99

IPCC (2007) Climate change 2007: the physical science basis. IPCC

Jones PD, Briffa KR, Osborn TJ, Lough JM, Van Ommen TD, Vinther BM, Luterbacher J, Wahl ER, Zwiers FW, Mann ME (2009) High-resolution palaeoclimatology of the last millennium: a review of current status and future prospects. Holocene 19:3

Li C, He J, Zhu J (2004) A review of decadal/interdecadal climate variation studies in China. Adv Atmos Sci 21:425–436

Li J, Chen F, Cook ER, Gou X, Zhang Y (2007) Drought reconstruction for north central China from tree rings: the value of the Palmer drought severity index. Int J Climatol 27:903–909

Li J, Cook ER, Chen F, Davi N, D'Arrigo R, Gou X, Wright WE, Fang K, Jin L, Shi J (2009) Summer monsoon moisture variability over China and Mongolia during the past four centuries. Geophys Res Lett 36:L22705. doi:10.1029/2009GL041162

Li J, Xie SP, Cook ER, Huang G, D'Arrigo R, Liu F, Ma J, Zheng XT (2011) Interdecadal modulation of El Niño amplitude during the past millennium. Nat Clim Chang 1:114–118

Liang E, Liu X, Yuan Y, Qin N, Fang X, Huang L, Zhu H, Wang L, Shao X (2006) The 1920s drought recorded by tree rings and historical documents in the semi-arid and arid areas of northern China. Clim Chang 79:403–432

Liu Y, Shi J, Shishov V, Vaganov E, Yang Y, Cai Q, Sun J, Wang L, Djanseitov I (2004) Reconstruction of May–July precipitation in

the north Helan Mountain, Inner Mongolia since AD 1726 from tree-ring late-wood widths. Chin Sci Bull 49:405–409
Lu R (2005) Interannual variation of North China rainfall in rainy season and SSTs in the equatorial eastern Pacific. Chin Sci Bull 50:2069–2073
Mantua NJ, Hare SR, Zhang Y, Wallace JM, Francis RC (1997) A Pacific interdecadal climate oscillation with impacts on salmon production. B Am Meteorol Soc 78:1069–1079
Meehl GA, Arblaster JM (2010) The tropospheric biennial oscillation and Asian-Australian monsoon rainfall. J Clim 15:722–744
Meko D (1997) Dendroclimatic reconstruction with time varying predictor subsets of tree indices. J Clim 10:687–696
Melvin TM, Briffa KR (2008) A signal-free approach to dendroclimatic standardisation. Dendrochronologia 26:71–86
Ni F, Cavazos T, Hughes MK, Comrie AC, Funkhouser G (2002) Cool-season precipitation in the southwestern USA since AD 1000: comparison of linear and nonlinear techniques for reconstruction. Int J Climatol 22:1645–1662
Pederson N, Jacoby GC, D'Arrigo RD, Cook ER, Buckley BM, Dugarjav C, Mijiddorj R (2001) Hydrometeorological reconstructions for Northeastern Mongolia derived from tree rings: 1651–1995. J Clim 14:872–881
Schiermeier Q (2010) The real holes in climate science. Nature 463:284–287
Shen C, Wang WC, Hao Z, Gong W (2007) Exceptional drought events over eastern China during the last five centuries. Clim Chang 85:453–471
Sontakke NA, Singh N (1996) Longest instrumental regional and all-India summer monsoon rainfall series using optimum observations: reconstruction and update. Holocene 6:315–331
Sontakke NA, Singh N, Singh HN (2008) Instrumental period rainfall series of the Indian region (AD 1813–2005): revised reconstruction, update and analysis. Holocene 18:1055–1066
Su M, Wang H (2006) Relationships between precipitation in China and ENSO. Science 36:951–958
Tan M, Liu T, Hou J, Qin X, Zhang H, Li T (2003) Cyclic rapid warming on centennial-scale revealed by a 2650-year stalagmite record of warm season temperature. Geophys Res Lett 30:1617–1620
Wang K, Wang P, Li Z, Cribb M, Sparrow M (2007) A simple method to estimate actual evapotranspiration from a combination of net radiation, vegetation index, and temperature. J Geophys Res 112:D15107. doi:15110.11029/12006JD008351
Wigley TML, Briffa KR, Jones PD (1984) Average value of correlated time series, with applications in dendroclimatology and hydrometeorology. J Appl Meteorol Clim 23:201–234
Wilmking M, D'Arrigo R, Jacoby GC, Juday GP (2005) Increased temperature sensitivity and divergent growth trends in circumpolar boreal forests. Geophys Res Lett 32. doi:10.1029/2005GL02333
Woodhouse CA (2001) A tree-ring reconstruction of streamflow for Colorado Front Range. J Am Water Resour Ass 37:561–569
Yang B, Braeuning A, Johnson KR, Yafeng S (2002) General characteristics of temperature variation in China during the last two millennia. Geophys Res Lett 29:1324. doi:10.1029/2001GL014485
Zhang R, Sumi A, Kimoto M (1999) A diagnostic study of the impact of El Nino on the precipitation in China. Adv Atmos Sci 16:229–241
Zhang Q, Hebda J, Alfaro I (2000) Modeling tree-ring growth responses to climatic variables using artificial neural networks. For Sci 46:229–239
Zhang P, Cheng H, Edwards RL, Chen F, Wang Y, Yang X, Liu J, Tan M, Wang X (2008) A test of climate, sun, and culture relationships from an 1810-year Chinese cave record. Science 322:940–942